A new algorithm for a better characterization and timing of the anti-VEGF vascular effect named “normalization”

Karima El Alaoui-Lasmaili, El-Hadi Djermoune, Jean-Baptiste Tylcz, Dominique Meng, François Plénat, Noémie Thomas, Béatrice Faivre

Journal:

Angiogenesis

Title:

A new algorithm for a better characterization and timing of the anti-VEGF vascular effect named "normalization"

Authors:

Karima El Alaoui-Lasmaili[1,2], El-Hadi Djermoune[1,2,4], Jean-Baptiste Tylcz[1,2], Dominique Meng[1,2], François Plénat[1,2,5,6], Noémie Thomas[1,2,4], Béatrice Faivre[1,2,3]

Authors affiliation:

[1]Université de Lorraine, CRAN, UMR 7039, Vandoeuvre-lès-Nancy, France

[2]CNRS, CRAN, UMR 7039, Vandoeuvre-lès-Nancy, France

[3]Université de Lorraine, Faculté de Pharmacie, Nancy

[4]Université de Lorraine, Faculté des Sciences et Techniques, Vandoeuvre-lès-Nancy

[5]Université de Lorraine, Faculté de Médecine, Vandoeuvre-lès-Nancy

[6]Laboratoire d'anatomopathologie, CHU Nancy-Brabois, Vandoeuvre-lès-Nancy

Corresponding author:

Pr. Béatrice Faivre (beatrice.faivre@univ-lorraine.fr)

Acknowledgements:

This work was supported by the research funds of the French Ligue Nationale Contre le Cancer, "Opération réalisée avec le concours financier du conseil régional de Lorraine" and Université de Lorraine

Abstract

Antiangiogenics are widely used in cancer treatment in combination to chemotherapy and radiotherapy for their vascular effects. Antiangiogenics are supposed to induce morphological and functional changes in the chaotic tumor vasculature that would help enhance the therapeutic efficacy of chemotherapy and radiotherapy through to the amelioration of the drug delivery or the oxygenation in the tumor, respectively. However, finding the best treatment sequence is not an easy task to achieve and no consensus has yet been established because of the lack of knowledge regarding when and for how long the vascular network is ameliorated.

The aim of this work was to develop a dedicated image processing algorithm able to analyze the vascular structures on optical microscopy images of the vascular network and to follow its fine modifications in vivo, over time. We applied this algorithm to follow the evolution of the vascular parameters (vascularized tissue surface, branches, sprouts and length), in response or not to anti-VEGF therapy (10 mg/kg/day) and determine precisely if there is really a vascular "normalization" with anti-VEGF therapy in comparison to the parameters extracted from healthy vascular networks.

We found that for this determination, the choice of region of interest to analyze is critical as it is important to compare only microcirculation areas and avoid areas with arteriole-venule-capillary hierarchy. The algorithm analysis allowed us to define a vascular “normalization” in treated tumors, between 8 and 12 days of bevacizumab treatment that was confirmed by standard immunohistochemical analysis, microvascular permeability assessment and immunohistological blood perfusion assessment.

Keywords:
Intravital imaging; Antiangiogenic therapy; Skinfold chamber; Algorithm quantification; Vascular normalization

1. Introduction

The use of antiangiogenic therapy in cancer was first based on the premise that antiangiogenic therapy could starve the tumor to death by reducing its blood supply [1]. Nevertheless, the tumor vasculature can be compared to the Braess paradox, as described by Kippenberger et al. [2] as the presence of a growing number of blood vessels resulting in too many vascular itineraries would reduce the efficiency of the tumor vascular network. The reduction of the vascular density by antiangiogenic therapy would not start by starving the tumor but instead could ameliorate the efficacy of the tumor vascular network [3] and hence be beneficial for tumor growth [4]. Thus, some authors underline the potential therapeutic benefit of antiangiogenic therapy because of the functional amelioration of the vascular network that would help enhance the therapeutic efficacy of chemotherapy and radiotherapy through to the amelioration of the drug delivery in the tumor or the oxygenation of tumor respectively [5]. Some of these described effects of the antiangiogenic agents are the modification of the shape of the blood vessels which appear thinner and less chaotic. The resulting vascular network would present a reduced vascular density associated to an enhanced pericyte coverage, a reduced permeability, and globally an ameliorated tumor perfusion and oxygenation [3]. This was hypothesized by Jain et al. [6] as being a tumor vascular “normalization” described by a transition of the morphology of the tumor blood vessels to a normal-like morphology.

However, if these vascular ameliorations named "normalization" are claimed by numerous authors, for anti-VEGF therapy there is still no consensus concerning when to administrate the bevacizumab (before, during or after chemotherapy or radiotherapy), at which posology (low or high dose, daily or not), and for how long as reviewed by Falk et al. [7]. Why the absence of a consensus? Because, to our knowledge the literature does not characterize what the real vascular effects of anti-VEGF agents are and for how long they are beneficial. Preclinical and clinical trials showed ambiguous and some paradoxical results as some studies demonstrate the importance of antiangiogenic agents in the global outcome [8, 9] when others do not [10–12]. A better knowledge of the vascular effects of bevacizumab would allow for a better and more secure use of it in the therapeutic protocols.

However, the access to that knowledge needs adequate tools capable of both exploring precisely the vascular effects of anti-VEGF therapy and determining when the administration and the duration of the treatment are more beneficial for an anti-tumor effect or to enhance the therapeutic efficacy of chemotherapy or radiotherapy. To our knowledge, there is no software able to quantify precisely the vasculature of tumors *in vivo*. Only softwares developed for *in vitro* angiogenesis analysis exist, such as Angiosys (TCS Cellworks, United Kingdom), AngioQuant, Angiogenesis analyzer for ImageJ or Wimasis [13, 14]. However, they are not robust enough as they do not permit a complete detection of the vascular network when blood vessels of various diameters coexist and when the architecture is too chaotic. Moreover, those softwares are not able to perform an automated analysis and lack precision so they are not utilizable to quantify and understand *in vivo* the evolution of the tumor vascular network through time.

In this context, the aim of our work was to develop a dedicated image processing algorithm able to detect and analyze the vascular structures on optical microscopy images of a vascular network and to follow its fine

modifications *in vivo*, over time. This dedicated image processing algorithm should allow to extract data from several pertinent vascular parameters (vascular and tissue surfaces, branches, sprouts and length) from images of the vascular network obtained *in vivo* by optical intravital microscopy observations of human glioblastoma xenografts implanted in skinfold chambers of *nude* mice. We applied this algorithm to follow the evolution of the vascular parameters in response or not to anti-VEGF therapy administrated daily at 10 mg/kg and determine precisely if there is really a vascular "normalization" with anti-VEGF therapy in comparison to the parameters extracted from healthy vascular networks. If it does, what parameter(s) attest it? when does the vascular amelioration happen? and for how long does it persist? The dedicated image processing algorithm and the robustness of the analysis of the vascular data was compared to immunohistochemical analysis and in addition to microvascular permeability assessment and immunohistological blood perfusion assessment.

2. Methods

2.1. Animals

All applicable institutional guidelines for the care and use of animals were followed. All procedures performed in this study were conducted in accordance with the European legislation for animal handling and with the approval of the local animal ethics committee (CELMEA-2012-0018). 8 to 10 weeks old *nude* female mice were used for the experiments (Janvier, France). Mice were housed separately once they had a skinfold chamber.

2.2. Dorsal skinfold chamber and glioblastoma xenografts implantation

Glioblastoma was chosen as a model of angiogenesis because it is a highly vascularized type of tumor [15, 16]. U87 xenografts were obtained and implantated in skinfold chambers as previously described in Tylcz et. al [17]. The dorsal skinfold chamber (APJ Trading) consists of two symmetrical titanium frames with a 1 cm^2 circle window of visualization. The mice were anesthetized by a single intraperitoneal injection of a mixture of xylazine (8 mg/kg, Rompun® 2%, Bayer Care Health) and ketamine (90 mg/kg, Imalgène® 500, Merial). To prevent post-operative pain and stress, mice were injected subcutaneously with a single dose of buprenorphine (0.05 mg/kg, Buprécare, Axience) and with a single dose of meloxicam (1 mg/kg, Metacam R, Boehringer Ingelheim) before the surgery.

24h to 48h post-surgery, a 3 +/- 1 mm^2 tumor fragment was placed directly on the vascular network inside the circular window of the chamber. The vascularization of the xenografts by the murine skin vessels was observed over time in microscopy.

2.3. Visualization of the vascular network in intravital microscopy

Bright field and fluorescence imaging of the vascular network of anesthetized mice bearing skinfold chambers was performed 3 to 6 times a week using the Nikon microscope AZ100 (Nikon, France) equipped with a Digital Light DS-Qi1Mc camera, with or without a confocal device (Revolution DSD, Andor Technology, United

Kingdom) and a TRITC filter (excitation wavelength = 560 +/- 25 nm). Depending on the experiment, the vascular network was observed with or without the preliminary injection of a contrasting agent (10 mg/kg of Texas Red-conjugated dextran, MW 70 000 Da, Fisher Scientific, France).

2.4. Bevacizumab treatment

After complete tumor vascularization (*i.e.* 10 to 14 days after the tumor implantation), 49 mice were divided into 6 lots: one lot without treatment (day 0) and 5 lots that received daily intraperitoneal injections of 10 mg/kg of bevacizumab (Avastin®, Roche) for 2, 4, 6, 10 or 14 days, respectively.

2.5. Experiments on tumor and healthy vascular networks

4 sets of experiments were conducted (Fig. 2). (i) 32 mice were treated or not with bevacizumab (10 mg/kg, daily) and used for intravital imaging, permeability assays and immunohistochemical quantification of the vascular markers chosen. In parallel, 8 mice remained untreated and were used for intravital imaging. (ii) 17 mice were treated or not with bevacizumab (10 mg/kg, daily) and used for the perfusion assessment. Moreover, 5 mice were used to image the healthy skin vascular network before the implantation of the tumor fragment.

2.6. Kinetic algorithmic quantification of the vascular parameters of the healthy and tumor vascular network on IVM images

In order to detect the vascular structures observed in intravital microscopy, we developed a dedicated image processing algorithm [17]. The algorithm first needs the definition and the localization of the region of interest (ROI) which was done using ImageJ (National Institutes of Health, Bethesda, MD, USA) [14] which size should give robust and fine information of the vascular network, independently of the tumor size and investigator. By comparison to the healthy vascular network, those information should allow the detection of the most discriminant and decisive parameters following the vascular remodeling in response or not to an antiangiogenic therapy to choose the best therapeutic protocol. Three types of ROI of different sizes were explored: ROI of 1 mm^2, 3 mm^2 and 10 to 14 mm^2 that gradually take into account the capillaries (microcirculation) or the capillaries and larger blood vessels. In healthy vascular networks, the bigger region of interest takes into account the arterioles, capillaries and venules. For each type of ROI, 3 measures at most were conducted and are represent by the mean +/- standard deviation for each data point.

Then the developed algorithm isolates the vasculature from the tissue by applying two first-order Savitzky-Golay filters (in the horizontal and vertical directions) to estimate the background which was subtracted from the original picture. The resulting image is then segmented by the same algorithm by detecting the wire-shaped structures that characterize the blood vessels (Fig. 1D). Each pixel constituting part of the blood vessels was counted to define the ratio V/T of the blood vessels surface (V) to the tissue (tumor or healthy tissue) surface analyzed (T) and its evolution was followed over time.

Starting from the segmented image, the skeleton of the vascular network is automatically obtained where all the vessels are replaced by unitary width lines to facilitate the quantification of the vascular sprouts, branching and total length. A vascular sprout is defined as a vascular segment of length between 5 and 50 pixels (*i.e.* 20 to 200 µm) with one free end and that is linked, on its other end, to a blood vessel. A vascular branch is defined as a structure composed of three segments sharing a common junction (just like the Y letter). For all the parameters, the quantification unit is the pixel. They are converted to µm using the fact that 1 pixel = 4.12 µm.

The number of branching and sprouts was studied either as the ratio to the tissue surface analyzed (branches/mm^2 and sprouts/mm^2 of tissue) or to the total vascular length (branches/mm and sprouts/mm of vessels) quantified within the region of interest (ROI). The total length was brought back to the surface of the tissue in mm^2 (length/mm^2 of tissue).

2.7. Microvascular permeability assessment with intravital microscopy

The functionality of the blood vessels was tested on mice of the lot (i) by analyzing whether the microvascular permeability was affected or not without and during bevacizumab treatment. Mice received an intravenous injection of dextran Texas Red® 70 kDa at 10 mg/kg (Fisher Scientific, France) 5 to 10 minutes before intravital imaging. The same areas of the tumors were imaged in fluorescence and in bright field. Fluorescence images were artificially colored in cyan in ImageJ software and were superimposed to the bright field images.

2.8. Immunohistological blood perfusion assessment

The functionality of the blood vessels was also tested by analyzing their capacity to perfuse the tumor tissue through the diffusion of Hoechst 33342 (25 mg/kg, i.v., 5 minutes before sacrifice, Molecular Probes, ThermoFisher Scientific, France) from the blood vessels to the surrounding tumor cells. On 6 µm frozen sections of the tumors, the blood vessels were detected with an anti-collagen IV antibody (rabbit polyclonal, 1/2000, #20451, Novotec) that was revealed with streptavidin-biotin complex method (secondary antibody: Goat polyclonal, 1/200, E0432, Dako; streptavidin - Fluoprobes 488, 1/8000, FP-BA2221, Fluoprobes, Interchim). Fluorescence images of the tumors were captured using AxioCam HRc camera on the Zeiss AxioImager.M1 with DAPI and FITC filters and analyzed with AxioVision Rel. 4.6 software (Carl Zeiss, France). Automatic mosaic acquisition was done for each tumor with each filter to detect both the cells stained with Hoechst 33342 and collagen IV. On ImageJ, the signal corresponding to the Hoechst 33342 and to the blood vessels were artificially colored in green and in red, respectively, to facilitate the distinction between perfused and non-perfused areas. Hematoxylin-Eosin-Saffron (HES) coloration was performed on all the tumors.

2.9. Immunohistological analysis

2.9.1. Immunohistochemical protocol for the tumors

At the different time points, the mice of the lot (i) were sacrificed and the tumors were fixed in formalin and embedded in paraffin. On 5 µm tumor sections, the blood vessels were detected with four different antibodies.

Anti-collagen IV (rabbit polyclonal, 1/2000, #20451, Novotec) staining was performed to detect the basement vascular membrane and to quantify the vascular density. Anti-CD105 (rat polyclonal, 1/30, CL8983AP, Cedarlane) to mark all activated endothelial cells. Anti-VEGFR-2 (rabbit polyclonal, 1/600, MA5-15556, Thermo Fischer Scientific) to mark only tip cells. Anti-desmin (mouse monoclonal, clone D33, Dako) to detect the accompanying cells, such as the pericytes. Each primary antibody was incubated with the tumor sections 1 night at +4°C. To detect anti-collagen IV and anti-VEGFR-2 antibodies, we used a method combining N-Histofine® Simple Stain Mouse (30 minutes, F/414341F, Microm Microtech) and a peroxidase substrate (ImmPACT NovarED, Eurobio). To detect anti-CD105 antibodies, the tumor sections were incubated with a biotinylated secondary antibody (1/800, 1 hour, 3052-08, Southern Biotech) that was revealed by a peroxidase conjugated to streptavidin (Streptavidine-HRP, 20 minutes, F/TS-125-HR, Microm Microtech) before incubation with the peroxidase substrate. To detect anti-desmin antibodies, a kit allowing the detection of mouse antibodies on mouse tissue was used (Mousestain Kit F/414321F, Microm Microtech). Finally, the sections were counterstained with Mayer's hematoxylin.

2.9.2. Quantification of the vascular parameters

Images of the tumors were captured using the Digital Light DS-Fi1 camera on the Nikon Eclipse E600 (Nikon, France). Mosaics of the whole tumors were made using the MosaicJ plugin of the Fiji software [18]. For each primary antibody, the number of blood vessels expressing the marker was counted on the entire surface to obtain a number of blood vessel/mm^2 of tumor.

The immunohistochemical quantification of the blood vessels on healthy vascular networks was performed on images of normal human skin biopsies marked with those antibodies. The images were selected from the Human Protein Atlas available from www.proteinatlas.org [19].

2.9.3. Detection of hypoxic zones

The hypoxic zones were detected by the expression of GluT-1 which was sought using an anti-GluT-1 antibody (rabbit polyclonal, 1/1000, E2844, Springbio) and a method combining N-Histofine® Simple Stain Mouse (30 minutes, F/414341F, Microm Microtech) and a peroxidase substrate (ImmPACT NovarED, Eurobio).

3. Results

To argue whether the vascular restructuring induced by bevacizumab corresponds to a vascular amelioration, named "normalization" (*i.e.* progression towards normal vascular structures) and if so, to determine the moment of apparition and the duration of the phenomenon, we characterize by using our dedicated algorithm the most judicious parameters and the most pertinent tissue area to analyze the vascular structural modifications induced by bevacizumab treatment and compare it to the healthy vascular networks of skins observed *in vivo* in skinfold chambers. The use of the skinfold chamber model permits the use of very few animals, over a period of 4 to 5 weeks, to obtain reliable and reproducible data, without having to sacrifice the mice.

3.1. Characterization of the structural modifications induced by bevacizumab treatment, *in vivo*, using our dedicated algorithm

3.1.1. The vascular data obtained depends on the choice of Region Of Interest (ROI)

By studying 3 sizes of regions of interest (ROI) on healthy and tumor vascular networks (1 mm^2, 3 mm^2 or 10-14 mm^2), we found that the information provided by the data analysis depended on the ROI studied. Indeed, for both tumor and healthy vascular networks, the quantification of the parameters (ratio V/T, branches/mm of vessel, sprouts/mm of vessel, branches/mm^2 of tissue, sprouts/mm^2 of tissue and length/mm^2 of tissue) was higher in smaller ROI compared to ROI of superior size. For example, the quantification of the parameter branches/mm of vessels was much superior in the microcirculation areas where only capillaries were considered, compared to intermediate and large areas where larger, poorly branched vessels were also considered (Fig. 3). Indeed, the arterioles and venules are less branched than the capillaries, hence the difference of pattern. Supplementary data Tables S1 and S2 confirm those observations for the other parameters studied for healthy and tumor vascular networks.

3.1.2. The ratio V/T permits to follow the evolution of the tumor vascularization

The overtime evolution of vascular networks in skinfold chambers of control or bevacizumab treated tumors is illustrated in figure 3A and 3B (top lines: intravital microscopy and bottom lines: after segmentation with the algorithm). From the segmentation, the algorithm determines the ratio V/T which corresponds to the ratio of the vascularized tumor surface to the tumor surface that were quantified over time for control (n = 8) and treated tumors (n = 7) to follow the evolution of the vascularization of the tumors in response to bevacizumab (10 mg/kg, daily).

The ratio V/T remained globally unchanged in control tumors during all of the experiment for all ROIs analyzed. This supposes that the tumor and vascular growth are correlated. On the contrary, in case of treatment, there was a lack of correlation between tumor and vascular growth and 3 phases of response could be highlighted. 1- From day 0 to day 6, the ratio V/T decreased due to the first effects of vascular growth inhibition by bevacizumab while the tumor surface was stabilizing. 2- Between day 6 and day 10, the ratio kept decreasing while the tumor

surface strongly increased, indicating a beneficial impact of the vascular remodeling to the tumor growth. 3- Between day 10 and day 14, the impact of the persistent vascular inhibition on the tumor growth appears with the new stabilization of tumor growth (Fig. 3C, 3D).
Compared to control tumors, the growth of the treated tumors was slightly improved, especially between day 8 and day 12 (Fig. 3D).
To evaluate if this ratio V/T could characterize a "normalization" phenomenon, this ratio was compared to the healthy tissues ratios for all ROIs studied (Fig. 3I, table 1). The ratio V/T in healthy tissue was not significantly different with non-treated tumors or after treatment, it was significantly lower in treated tumors compared to healthy tissues.
The evolution of the vascularization in tumors treated or not in regards of the tumor growth leads us to suspect a really efficient vascular remodeling with bevacizumab. But the ratio V/T in all ROIs compared to healthy tissues was not an adequate parameter to affirm of a vascular normalization" phenomena and to determine precisely when and for how long it appears.

3.1.3. Characteristics of the vascular network pattern associated with the vascular "normalization"

To know if and when the vascular remodeling due to the angiogenesis inhibition (reduction of the sprouting) and the anti-vascular effect (reduction of the number of vascular branches and of vascular length) could be considered as a progress towards normal vascular structures, we analyzed when treated tumor data was significantly different from control data and when it matched with healthy tissue data (Fig. 4, Table 1).

All of the parameters analyzed had a globally constant stability in control tumors for all ROIs analyzed and they decreased significantly over time in treated tumors. For all three ROIs analyzed, the curves of evolution of the vascular branches, sprouts and length/mm^2 of tissue followed the same decrease (Fig. 4, Table 1). For all three parameters, the most significant differences between control and treated data was observed between day 8 and day 12 when the tumor growth started again. This was correlated with a global decrease of the sprouts, branches and vascular length per surface of tumor.
The matches with healthy data were possible mainly only on the microcirculation ROIs and started at day 8. More precisely, when brought back to the total vascular length, the branches (branches/mm of vascular length) were practically similar within the microcirculation and intermediate area but they were not discriminant from control tumors when studied in large areas. Between day 8 and up to day 14, the quantification of the branches, sprouts and length of the vascular network matched the microcirculation of healthy tissue. This suggests that the structural amelioration of the treated tumor vascular network occurs during the second week of treatment and is more pronounced precisely between day 9 and day 12. On the other hand, when focusing on the intermediate and large areas, the vascular parameters of treated tumors remained different from those quantified in the healthy vascular networks because the blood vessels were larger and structured according to the arteriole-venule-capillary hierarchy found in normal vascular networks but not in tumors.

3.2. Immunohistochemical analysis versus algorithmic analysis

Immunostaining of VEGFR-2, CD105, collagen IV and desmin of treated tumors at different time points and of healthy tissue was used to validate the *in vivo* algorithm analysis (Fig. 5, Table S3). First, we analyzed how bevacizumab treatment affects the expression of those markers by the blood vessels over time and when it matched with healthy data. The number of blood vessels marked by type IV collagen and VEGFR-2 were very high in the tumors without treatment at day 0 (158 +/- 27 and 139 +/- 23 blood vessels/mm^2, respectively). However, fewer vessels were counted with CD105 and desmin stainings (82 +/- 36 and 84 +/- 25 blood vessels/mm^2, respectively). In the first 6 days of treatment, the number of blood vessels marked by VEGFR-2, CD105, desmin and type IV collagen decreased and all progressed towards a stabilization up to the end of the experiment.

All of those markers followed the same tendency as the parameters quantified with the algorithm after the start of bevacizumab treatment. They all underwent a decrease due to the antiangiogenic and anti-vascular effects and progressed towards a stabilization state. Each parameter quantified in immunohistochemistry in tumors matched with healthy tissue at different periods. CD105 and collagen IV stained blood vessels reached values of healthy tissue at day 2 and 4, respectively. However, this was not during the stabilization state observed previously. VEGFR-2 labeled blood vessels reached by day 6 normal values of healthy tissues and remained this way up to day 14. The number of desmin-labeled blood vessels between day 4 and day 14 fluctuated but reached values of healthy tissue by day 10.

All four parameters confirm the evolution observed and quantified with the algorithm with a common steady state that occurs between day 8 and day 12 during which the endothelial sprouting (VEGFR-2) and the pericyte coverage (desmin) reached healthy values.

3.3. Vascular functional parameters analyses

To find out if the vascular amelioration characterized is functionally confirmed, we studied if and how the functionality of the blood vessels was affected during bevacizumab treatment, *in vivo* by studying their permeability and *ex vivo* by evaluating both their tissue perfusion capacity and tissue hypoxia (Fig. 6). Although the vascular network at day 0 appears composed of tortuous and dense blood vessels both in intravital microscopy and in immunohistochemistry (Fig. 3 and 5), the diffusion of Hoechst 33342 shows that the tumors were completely perfused (Fig. 6A and 6B). No dextran leakage was observable and thrombi in the blood vessels were rare.

At day 2, during the first effects of the vascular inhibition by bevacizumab, Hoechst 33342 perfusion in the treated tumor was heterogeneous and the areas lacking perfusion coincided with the presence of occlusive thrombi in the blood vessels and edema in the tumor tissue on HES-colored tumors (Fig. 6A). At 2 and 5 days of bevacizumab treatment, dextran leakage was observed locally in the tumor. By day 6, the perfusion was qualitatively better but large non-perfused areas were still present and associated with the presence of thrombi and edema.

By day 10, the perfusion was qualitatively better and the tumor tissue did not present any edema or thrombi. However, at day 14, intravital microscopy showed that more than half of the blood vessels were damaged leaving empty sleeves of vessels and potential thrombi that can further stimulate angiogenesis (Fig. 6D). Between 6 and 14 days of treatment, the blood vessels showed no extravasation of dextran.

The expression of the glucose transporter GluT-1, used to reveal hypoxia areas, was highly and uniformly expressed in the tumors at day 0 although at the same stage, tumors were well-perfused (Fig. 6C). After 2 days of bevacizumab treatment, the expression of GluT-1 decreased but remained homogeneously distributed in all of the tumor tissue. The expression of GluT-1 was reduced and inhomogeneous from day 6 to day 14, with a more pronounced decrease by day 10, indicating that hypoxia was alleviated in the tumors.

4. Discussion

The aim of this work was to introduce a new method to identify precisely the period of vascular amelioration induced by anti-VEGF therapy in order to improve their use in therapeutic protocols. To figure out when the vascular remodeling induced by the anti-VEGF treatment could be qualified as a vascular "normalization", the evolution of the fine changes in the blood vessels, in their sprouting capacity and in their branching pattern was evaluated in tumor and healthy vascular networks to search for the most discriminant parameters of the vascular "normalization".

The analysis of different ROIs shows that only the microcirculation area, where the vascular hierarchy (arteriole-capillary-venule) is not taken into account, could demonstrate a match between healthy and tumor vascular data allowing to prove the existence of a real progression towards normal vascular structures in response to bevacizumab (10 mg/kg, daily). In treated tumor vascular networks, with bevacizumab the normal vascular hierarchy can never be reached considering the speed of vascular remodeling and the destabilization of the angiogenic balance (not only VEGF-dependent).

A primary exploration of the tumor vascularized surface (parameter V/T), showed that the vascular remodeling imposed by bevacizumab did reduce the quantity of blood vessels but did not inhibit the growth of tumors. This point is in favor of the amelioration of the vascular network that occurs between 8 and 12 days of bevacizumab treatment and is in agreement with the findings by Grepin et al. [4] where bevacizumab treatment enhances tumor growth. However, no correlation with the healthy V/T could be shown which means that this parameter is not robust enough to detect the vascular “normalization” and it is not a discriminant parameter. The non-different high values of V/T in the healthy and tumor tissue could be respectively the result of the presence of big blood vessels in the healthy tissue and the presence of a large number of neovessels in the tumor tissue that compensate for the surface of the healthy blood vessels.

The quantification of the branches/mm^2 of tissue surface or /mm of vascular length in the microcirculation area (Fig. 4 and table 1) are the most robust and discriminant parameters to detect the time-lapse when the vascular remodeling of the tumor vascular network can be considered as a vascular "normalization". The comparison to the healthy vascular network shows that the tumor vascular network is structurally ameliorated starting from day 8 of bevacizumab treatment (10 mg/kg, daily) until day 12, when the vascular remodeling is not favorable anymore to tumor growth.

As for the other parameters studied (sprouts/mm of vessel, sprouts/mm^2 of tissue), their matching with healthy data is not correlated to an efficient vascular remodeling period and thus are not discriminant parameters of the vascular “normalization” (Table 1, Tables S1 and S2).

The *in vivo* algorithmic analysis was confirmed using standard immunohistochemistry techniques. The morphological features of the blood vessels such as their organization in clusters characteristic of highly angiogenic tumors, disappeared with the therapy leaving straighter vessels. This observation is consistent with existing data and with the concept of the vascular "normalization" [3, 20]. We showed that mature and immature blood vessels are pruned during bevacizumab treatment. We chose CD105 to stain the blood vessels because it is expressed on activated endothelial cells [21], so its staining should allow the visualization of the tip cells and the stalk cells. Without treatment we could not count as much CD105 stained blood vessels as type IV collagen which suggest that the tumor vascular network is not only composed by activated endothelial cells but also by a portion of phalanx cells possibly composing mature vessels. This would imply that half of the blood vessels are activated and thus probably immature while the other half is possibly mature and stable and both are pruned during bevacizumab therapy. Sprouting blood vessels detected by VEGFR-2, known to be overly expressed on tip cells [22], decreased during the treatment which suggests that the endothelial sprouting is reduced but not stopped. The decrease of both VEGFR-2 labeled blood vessels and the vascular sprouts is representative of the antiangiogenic effect of bevacizumab while the decrease of both type IV collagen stained blood vessels and the vascular branches is representative of the anti-vascular effect of bevacizumab.

Our algorithmic analyses of the sprouts, branches and length shows the antiangiogenic and anti-vascular effects like immunohistochemical analyses do. The immunohistochemical quantification of the tumor blood vessels marked with type IV collagen and CD105 (Fig. 5) could not show a resemblance to healthy vascular networks during the stabilization period and hence are not considered as discriminant parameters of the vascular "normalization". The analysis of VEGFR-2 and desmin marked blood vessels shows better correlation between tumor and healthy vascular networks during the stabilization period. However, unlike with our algorithm, the impossibility to define a ROI limited to the microcirculation (*i.e.* capillaries) renders the comparison between tumor and healthy vascular networks in immunohistochemistry misleading and perhaps poorly representative of the vascular "normalization". Moreover, this algorithm would allow to overcome of the technical problems encountered in immunohistochemistry where the quantification of the vascular density is subjective because it depends on the quality of the coloration, on the experimenter and on how the blood vessels are sectioned [23].
The use of the algorithm to follow the tumor response to antiangiogenic therapy in the same animal, over time, resulted in a more precise determination of the treatment response than immunohistochemsitry alone while using less animals (7 *vs* 24, respectively).

We have demonstrated that the vascular remodeling with bevacizumab administrated daily at 10 mg/kg is beneficial for tumor growth only between day 8 and day 12 of treatment. The quantification of the branches features a beneficial state between 8 and 12 days of bevacizumab treatment and appears as a discriminant parameter of the vascular “normalization”. In that state, 20% to 40% of the quantity of blood vessels initially present remains. Tolaney et al. suggest that a high baseline microvascular density may be necessary to go

through a "normalized" state and not go directly into excessive vascular pruning [21]. In our experiments, bevacizumab treatment was started when the vascularized tumor surface was at its maximum and despite of the massive doses of anti-VEGF therapy administrated, angiogenesis is not fully inhibited but rather moderated. This suggests that the remaining 20% of microvascular density and vascular branches are enough and better structured to allow for tumor regrowth.
Considering the vascular parameters extracted from the skeletonization of the images with the dedicated algorithm, the sprouts/mm^2 of tissue surface or /mm of vascular length (Fig. 4 and Table 1) were not appropriate to confirm of an efficient vascular remodeling nor of a vascular "normalization". The study of the sprouting *via* VEGFR-2 expression (in immunohistochemistry) and *via* the algorithm quantification is not a discriminant parameter to conclude of a vascular "normalization" phenomenon with bevacizumab treatment.

Correspondingly to *in vivo* observations and quantification of the vascular parameters, the tumor vasculature underwent a rapid breakdown starting from 2 days of treatment that had an impact on tumor growth. The first responses to bevacizumab are the antiangiogenic and anti-vascular effects causing the blood vessels to leak hence triggering the formation of thrombi that obstruct the blood vessels. The presence of thrombin might add to the anti-vascular effect as it induces the disruption of the endothelial barrier [22] which potentially increases the permeability and leads to blood leakage. This provokes the formation of edemas that prevents the blood to perfuse the entire tumor tissue because of the elevated interstitial pressure [24]. Hence it probably results in the development of highly hypoxic regions (where GluT-1 was overexpressed) and presenting some small necrotic areas. In response, a vascular remodeling occurs between days 6 and 10, that does not significantly modifies the number of blood vessels but reorganizes them to obtain a vascular network that is less chaotic and less branched. Thus, the blood irrigation within the tumor tissue is reestablished that leads to a less hypoxic tissue and a better tumor growth. By day 14, the excess of anti-VEGF resulted in a strong vascular regression. Hypoxia is restored in some places and tumors grow very slowly.

In conclusion, our algorithm stands as a sufficiently reliable and robust mathematical tool to characterize, from optical microscopy images, the vascular remodeling in response to bevacizumab treatment and to detect when the remodeling is efficient enough to assure that the functionality of the blood vessels is restored *via* a more efficient blood circulation in the tumor, less vascular permeability, better tissue oxygenation and a better perfusion. The analysis of the vascular networks must be limited to the microcirculation area, *i.e.* capillaries where the most discriminant parameter of the vascular "normalization" are the branches/mm^2 of tissue surface or /mm of vascular length. The algorithmic analysis of those two parameters on healthy vascular networks compared to tumor vascular networks confirmed a real "normalizing" effect of bevacizumab. At the dose of 10 mg/kg daily, the "normalization" effect of the neovascularization of glioblastoma xenografts in mice was obtained after 8 days of therapy and lasted 4 to 5 days.
In our conditions, in order to optimize chemotherapy and radiotherapy based protocols, it would seem optimal to start chemotherapy or radiotherapy 8 days after the start of daily bevacizumab therapy.

Perspectives

The method and algorithmic analysis developed here will have to be used to determine, *in vivo* in different types of tumors, the dose and duration of bevacizumab treatment required for its association to chemotherapy or radiotherapy to maximize their therapeutic efficacy. It will also be studied in a manner to predict the best protocol of administration of anti-VEGF to use in order to ensure, in the future, an optimal antitumor response in patients.

Conflicts of interest. The Authors declare that they have no conflicts of interest.

1. Folkman J (1972) Anti-angiogenesis: new concept for therapy of solid tumors. Ann Surg 175:409–416.

2. Kippenberger S, Meissner M, Kaufmann R, Hrgovic I, Zöller N, Kleemann J (2016) Tumor Neoangiogenesis and Flow Congestion: A Parallel to the Braess Paradox? Circ Res 119:711–713. doi: 10.1161/CIRCRESAHA.116.309411

3. Goel S, Duda DG, Xu L, Munn LL, Boucher Y, Fukumura D, Jain RK (2011) Normalization of the Vasculature for Treatment of Cancer and Other Diseases. Physiol Rev 91:1071–1121. doi: 10.1152/physrev.00038.2010

4. Grepin R, Guyot M, Jacquin M, Durivault J, Chamorey E, Sudaka A, Serdjebi C, Lacarelle B, Scoazec J-Y, Negrier S, Simonnet H, Pages G (2012) Acceleration of clear cell renal cell carcinoma growth in mice following bevacizumab/Avastin treatment: the role of CXCL cytokines. Oncogene 31:1683–1694. doi: 10.1038/onc.2011.360

5. Goel S, Wong AH-K, Jain RK (2012) Vascular normalization as a therapeutic strategy for malignant and nonmalignant disease. Cold Spring Harb Perspect Med 2:a006486. doi: 10.1101/cshperspect.a006486

6. Jain RK (2001) Normalizing tumor vasculature with anti-angiogenic therapy: A new paradigm for combination therapy. Nat Med 7:987–989. doi: 10.1038/nm0901-987

7. Falk AT, Barrière J, François E, Follana P (2015) Bevacizumab: A dose review. Crit Rev Oncol Hematol 94:311–322. doi: 10.1016/j.critrevonc.2015.01.012

8. Hurwitz H, Fehrenbacher L, Novotny W, Cartwright T, Hainsworth J, Heim W, Berlin J, Baron A, Griffing S, Holmgren E, Ferrara N, Fyfe G, Rogers B, Ross R, Kabbinavar F (2004) Bevacizumab plus Irinotecan, Fluorouracil, and Leucovorin for Metastatic Colorectal Cancer. N Engl J Med 350:2335–2342. doi: 10.1056/NEJMoa032691

9. McGee MC, Hamner JB, Williams RF, Rosati SF, Sims TL, Ng CY, Gaber MW, Calabrese C, Wu J, Nathwani AC, Duntsch C, Merchant TE, Davidoff AM (2010) Improved Intratumoral Oxygenation Through Vascular Normalization Increases Glioma Sensitivity to Ionizing Radiation. Int J Radiat Oncol 76:1537–1545. doi: 10.1016/j.ijrobp.2009.12.010

10. Arjaans M, Oude Munnink TH, Oosting SF, Terwisscha van Scheltinga AGT, Gietema JA, Garbacik ET, Timmer-Bosscha H, Lub-de Hooge MN, Schroder CP, de Vries EGE (2013) Bevacizumab-Induced Normalization of Blood Vessels in Tumors Hampers Antibody Uptake. Cancer Res 73:3347–3355. doi: 10.1158/0008-5472.CAN-12-3518

11. Dobosz M, Ntziachristos V, Scheuer W, Strobel S (2014) Multispectral Fluorescence Ultramicroscopy: Three-Dimensional Visualization and Automatic Quantification of Tumor Morphology, Drug Penetration, and Antiangiogenic Treatment Response. Neoplasia N Y N 16:1–13.

12. Goldwirt L, Beccaria K, Carpentier A, Idbaih A, Schmitt C, Levasseur C, Labussiere M, Milane A, Farinotti R, Fernandez C (2015) Preclinical impact of bevacizumab on brain and tumor distribution of irinotecan and temozolomide. J Neurooncol 122:273–281. doi: 10.1007/s11060-015-1717-1

13. Carpentier G (2012) Angiogenesis Analyzer for ImageJ.

14. Schindelin J, Rueden CT, Hiner MC, Eliceiri KW (2015) The ImageJ ecosystem: An open platform for biomedical image analysis. Mol Reprod Dev 82:518–529. doi: 10.1002/mrd.22489

15. Das S, Marsden PA (2013) Angiogenesis in Glioblastoma. N Engl J Med 369:1561–1563. doi: 10.1056/NEJMcibr1309402

16. Keunen O, Johansson M, Oudin A, Sanzey M, Rahim SAA, Fack F, Thorsen F, Taxt T, Bartos M, Jirik R, Miletic H, Wang J, Stieber D, Stuhr L, Moen I, Rygh CB, Bjerkvig R, Niclou SP (2011) Anti-VEGF

treatment reduces blood supply and increases tumor cell invasion in glioblastoma. Proc Natl Acad Sci 108:3749–3754. doi: 10.1073/pnas.1014480108

17. Tylcz J-B, El Alaoui-Lasmaili K, Djermoune E-H, Thomas N, Faivre B, Bastogne T (2015) Data-driven modeling and characterization of anti-angiogenic molecule effects on tumoral vascular density. Biomed Signal Process Control 20:52–60. doi: 10.1016/j.bspc.2015.04.008

18. Schindelin J, Arganda-Carreras I, Frise E, Kaynig V, Longair M, Pietzsch T, Preibisch S, Rueden C, Saalfeld S, Schmid B, Tinevez J-Y, White DJ, Hartenstein V, Eliceiri K, Tomancak P, Cardona A (2012) Fiji: an open-source platform for biological-image analysis. Nat Methods 9:676–682. doi: 10.1038/nmeth.2019

19. Uhlén M, Fagerberg L, Hallström BM, Lindskog C, Oksvold P, Mardinoglu A, Sivertsson Å, Kampf C, Sjöstedt E, Asplund A, Olsson I, Edlund K, Lundberg E, Navani S, Szigyarto CA-K, Odeberg J, Djureinovic D, Takanen JO, Hober S, Alm T, Edqvist P-H, Berling H, Tegel H, Mulder J, Rockberg J, Nilsson P, Schwenk JM, Hamsten M, von Feilitzen K, Forsberg M, Persson L, Johansson F, Zwahlen M, von Heijne G, Nielsen J, Pontén F (2015) Proteomics. Tissue-based map of the human proteome. Science 347:1260419. doi: 10.1126/science.1260419

20. Fischer I, Cunliffe CH, Bollo RJ, Raza S, Monoky D, Chiriboga L, Parker EC, Golfinos JG, Kelly PJ, Knopp EA, Gruber ML, Zagzag D, Narayana A (2008) High-grade glioma before and after treatment with radiation and Avastin: initial observations. Neuro-Oncol 10:700–708. doi: 10.1215/15228517-2008-042

21. Tolaney SM, Boucher Y, Duda DG, Martin JD, Seano G, Ancukiewicz M, Barry WT, Goel S, Lahdenrata J, Isakoff SJ, Yeh ED, Jain SR, Golshan M, Brock J, Snuderl M, Winer EP, Krop IE, Jain RK (2015) Role of vascular density and normalization in response to neoadjuvant bevacizumab and chemotherapy in breast cancer patients. Proc Natl Acad Sci 112:14325–14330. doi: 10.1073/pnas.1518808112

22. Ashina K, Tsubosaka Y, Kobayashi K, Omori K, Murata T (2015) VEGF-induced blood flow increase causes vascular hyper-permeability in vivo. Biochem Biophys Res Commun 464:590–595. doi: 10.1016/j.bbrc.2015.07.014

23. de Matos LL, Trufelli DC, de Matos MGL, da Silva Pinhal MA (2010) Immunohistochemistry as an Important Tool in Biomarkers Detection and Clinical Practice. Biomark Insights 5:9–20.

24. Padera TP, Stoll BR, Tooredman JB, Capen D, di Tomaso E, Jain RK (2004) Pathology: cancer cells compress intratumour vessels. Nature 427:695. doi: 10.1038/427695a

Journal:

Angiogenesis

Title:

A new algorithm for a better characterization and timing of the anti-VEGF vascular effect named "normalization"

Authors:

Karima El Alaoui-Lasmaili[1,2], El-Hadi Djermoune[1,2,4], Jean-Baptiste Tylcz[1,2], Dominique Meng[1,2], François Plénat[1,2,5,6], Noémie Thomas[1,2,4], Béatrice Faivre[1,2,3]

Authors affiliation:

[1]Université de Lorraine, CRAN, UMR 7039, Vandoeuvre-lès-Nancy, France

[2]CNRS, CRAN, UMR 7039, Vandoeuvre-lès-Nancy, France

[3]Université de Lorraine, Faculté de Pharmacie, Nancy

[4]Université de Lorraine, Faculté des Sciences et Techniques, Vandoeuvre-lès-Nancy

[5]Université de Lorraine, Faculté de Médecine, Vandoeuvre-lès-Nancy

[6]Laboratoire d'anatomopathologie, CHU Nancy-Brabois, Vandoeuvre-lès-Nancy

Corresponding author:

Pr. Béatrice Faivre (beatrice.faivre@univ-lorraine.fr)

Acknowledgements:

This work was supported by the research funds of the French Ligue Nationale Contre le Cancer, "Opération réalisée avec le concours financier du conseil régional de Lorraine" and Université de Lorraine

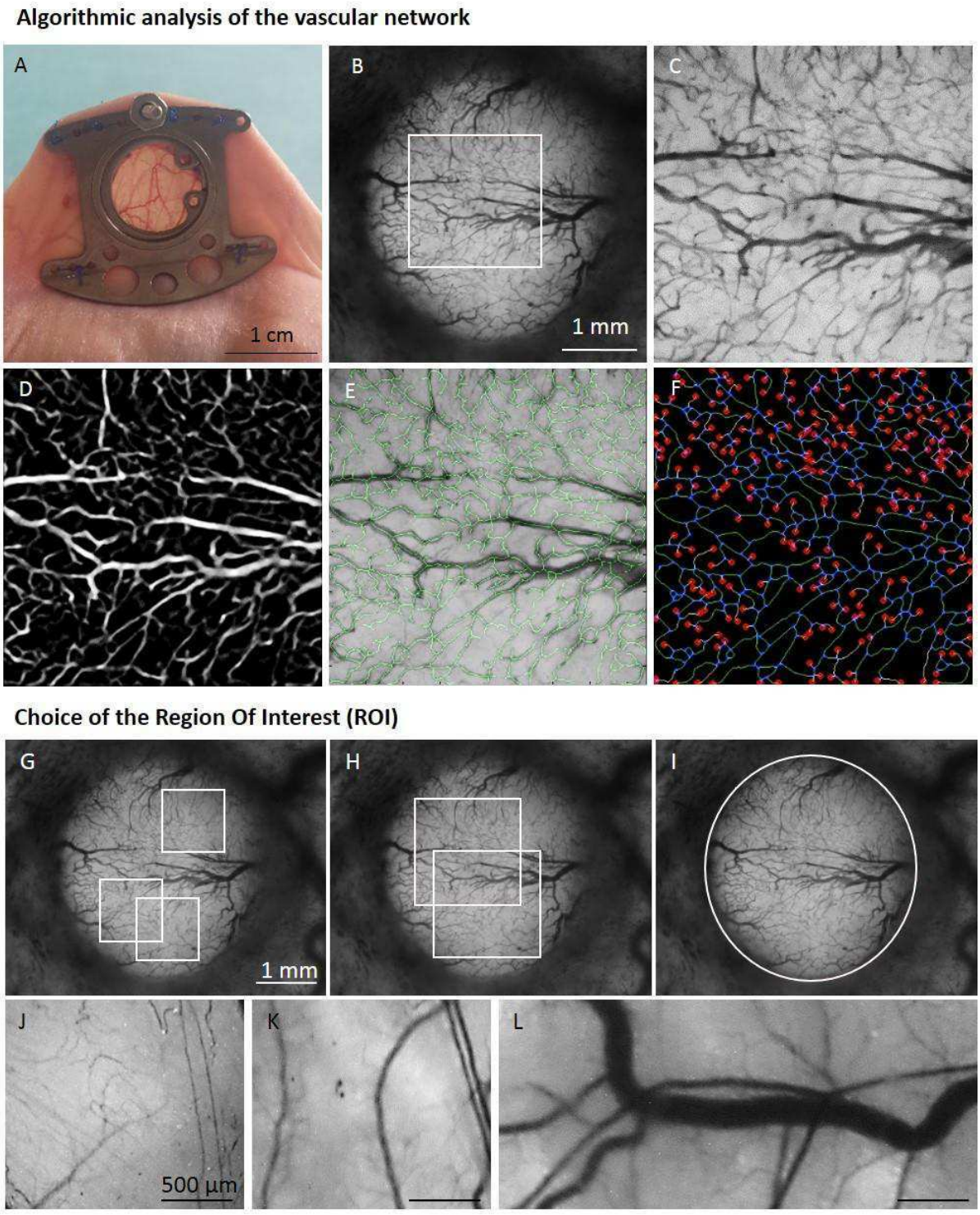

Fig. 1 Algorithmic analysis of the vascular network on intravital microscopy images of tumors implanted in skinfold chambers of mice. a A skinfold chamber implanted on the back of a nude mouse allowing the visualization of the skin's vascular network. **b** Example of a tumor 11 days after its implantation in the chamber and observed in bright field microscopy. A region of interest was selected and enlarged in (**c**) to better visualize the steps of the analysis. **d** The image is segmented to extract specifically the blood vessels because of their tubular shape. **e** A skeleton of the vasculature (in green) is made on the vascular network which allows for (**f**) the quantification of the length, branches (blue) and sprouts (yellow) of the blood vessels. **Choice of the Region Of Interest (ROI)** Three different regions of interest of different sizes were chosen for tumor (**g,h,i**) and healthy (**j,k,l**) vascular networks including (**g,j**) the microcirculation (1 mm^2), (**h,k**) the microcirculation and larger

vessels (intermediate area of 3 mm^2) or (**i,l**) all kind of vessels (large area of 10 to 14 mm^2). Each area was analyzed at most three times.

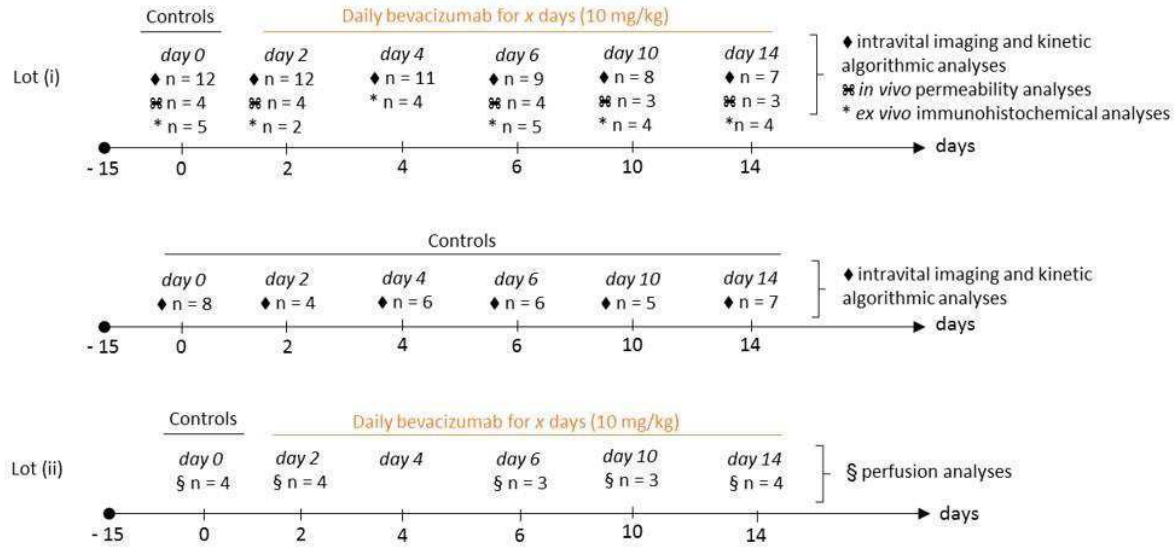

Fig. 2 Chronology of the experiments. 3 sets of experiments were conducted on nude mice bearing skinfold chambers with a U87 glioblastoma tumor fragment. Bevacizumab therapy was started for all the mice at day 0, when the tumor surface appeared completely vascularized in intravital microscopy. (i) 32 mice were treated or not with bevacizumab (10 mg/kg, daily) and used for intravital imaging, permeability assays and immunohistochemical quantification of the vascular markers chosen. In parallel, 8 mice remained untreated and were used for intravital imaging. The tumors were fixed in formalin at the different time-points for immunohistochemistry analyses. (ii) 17 mice were treated or not with bevacizumab (10 mg/kg, daily) and used for the perfusion assessment. The tumors were snap-frozen at the different time-points for perfusion analyses (iii) 5 mice were used to image the healthy skin vascular network before the implantation of the tumor fragment.

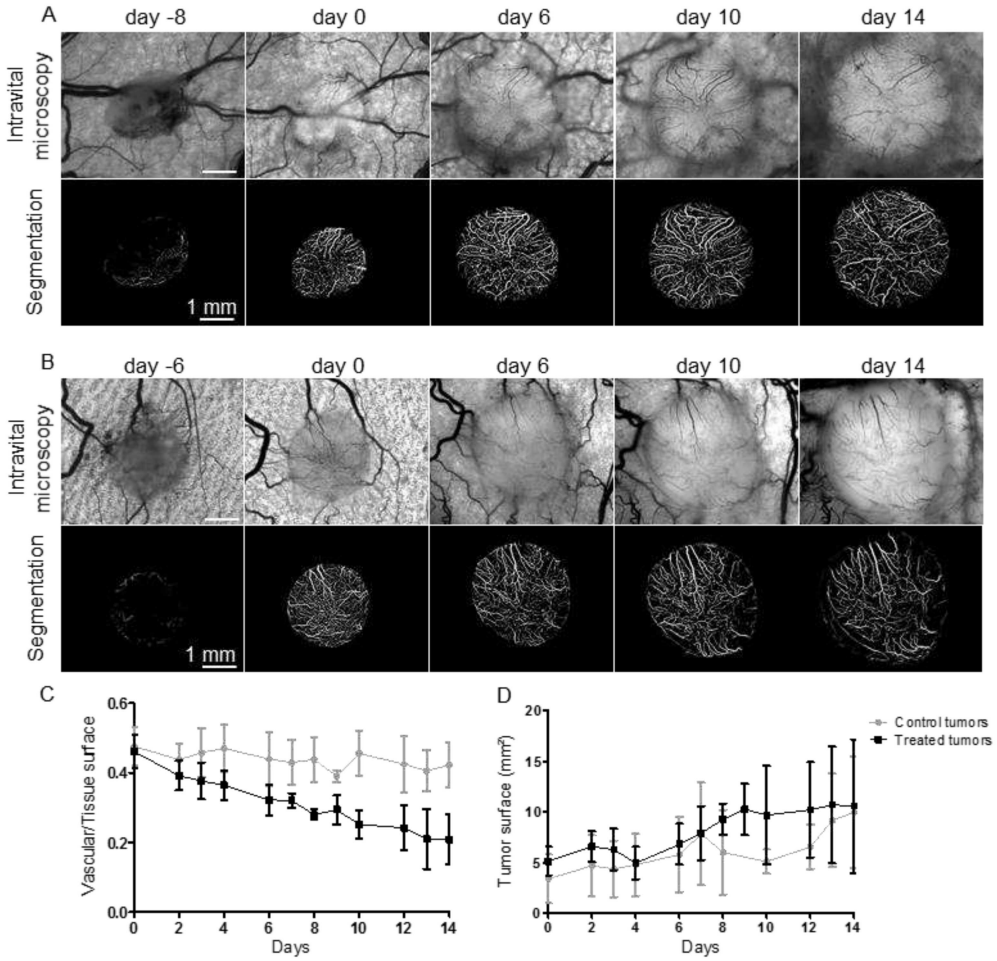

Fig. 3 Evolution of the vascular networks of two tumors in intravital microscopy and after segmentation. U87 glioblastoma tumor fragments were implanted in the skinfold chambers of *nude* mice and their vascularization was monitored by intravital microscopy from the implantation of the tumor fragment to the end of the protocol. Day 0 that was defined as the beginning of the treatment is the day when the tumor surface appears completely irrigated by the blood vessels (tumor vascularized). **a** Example of a tumor left untreated, at day-8, the tumor fragment had been deposited for 5 days. **b** Example of a tumor treated with bevacizumab daily at 10 mg/kg starting from day 0. At day-6, the tumor fragment had been implanted for 5 days. **c** Ratio of the total vascular length in mm per surface of tissue analyzed in mm^2 quantified on the large ROI on the segmentation images for control (grey, n = 8) and treated (dark, n = 7) tumors. **d** Tumor growth of control and treated tumors represented by the measure of the tumor surfaces. Each data point represents the mean +/- SD of those measures.

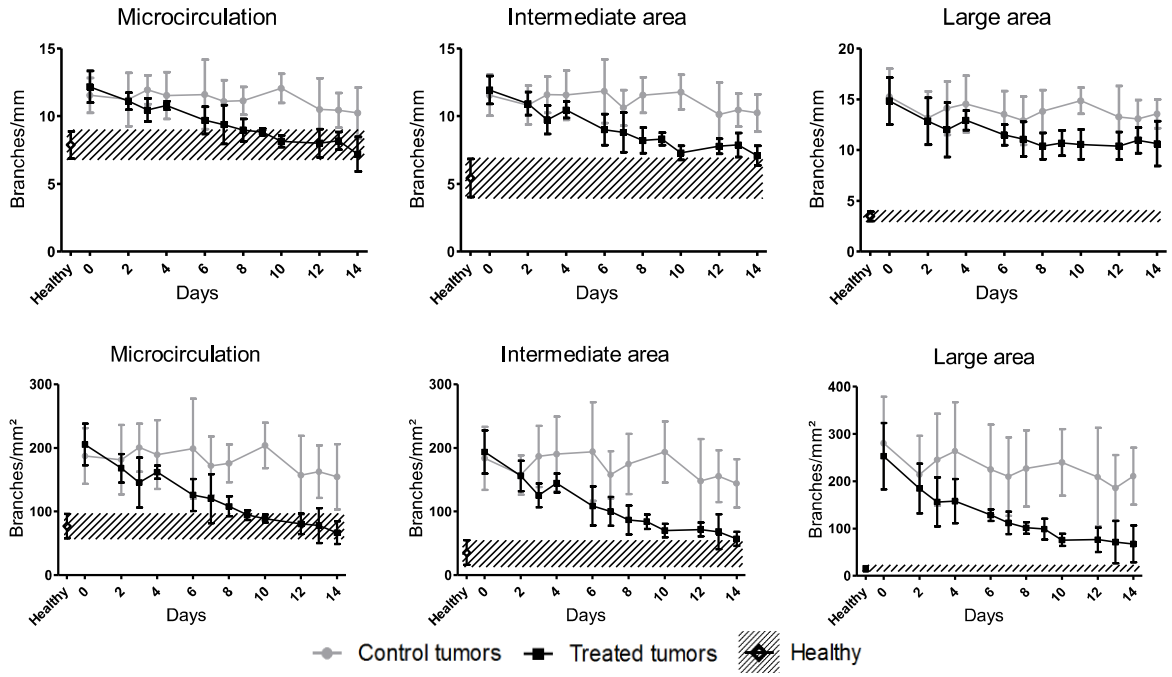

Fig. 4 Branching pattern in control and treated tumors and comparison to healthy tissue. The number of branching points was quantified on the skeleton of the vascular networks issued from the segmentation images by defining a branch as a structure composed of three segments sharing a common junction (just like the Y letter). The number of branching points was studied as its ratio to the total vascular length (branches/mm of vessels, graphs on top) and as its ratio to the tissue surface analyzed (branches/mm^2 of tissue surface, graphs on the bottom). Those ratios were analyzed for three different regions of interest of different sizes for tumor and healthy vascular networks including the microcirculation (1 mm^2), the microcirculation and larger vessels (intermediate area of 3 mm^2) and all kind of vessels (large area of 10 to 14 mm^2). Healthy data is represented as the mean of 5 measures in the hatched area to facilitate the comparison to control (grey lines, n = 8) and treated (dark lines, n = 7) tumor data. Each area was analyzed at most three times and each data point represents the mean +/- SD of those measures.

Table 1: Identification of the period during which the vascular parameters quantified on the treated tumor vascular networks match those quantified on healthy vascular networks, in the three regions of interests (microcirculation, intermediate area and large area).

	Matches	*Healthy vascular networks*		
	Treated vascular networks	*Microcirculation*	*Intermediate area*	*Large area*
Branches/mm	*Microcirculation*	day 8 to 12	-	-
	Intermediate area	-	never	-
	Large area	-	-	never
Sprouts/mm	*Microcirculation*	day 13	-	-
	Intermediate area	-	never	-
	Large area	-	-	never
Length/mm^2	*Microcirculation*	day 9 to 12	-	-
	Intermediate area	-	never	-
	Large area	-	-	never
Branches/mm^2	*Microcirculation*	day 9 to 12	-	-
	Intermediate area	-	day 14	-
	Large area	-	-	never
Sprouts/mm^2	*Microcirculation*	day 12	-	-
	Intermediate area	-	never	-
	Large area	-	-	never
Ratio V/T	*Microcirculation*	day 0	-	-
	Intermediate area	-	day 2 to 7	-
	Large area	-	-	day 2 to 3

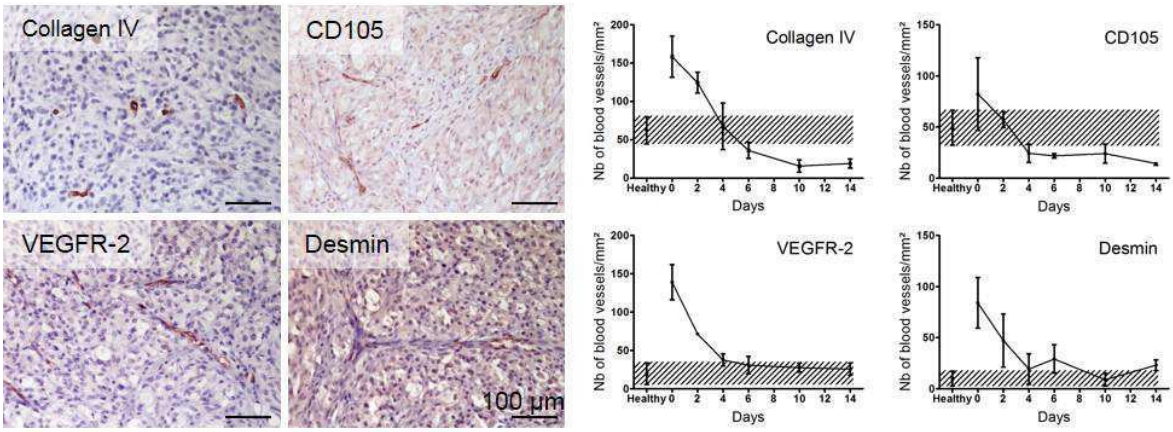

Fig. 5 Immunohistochemical analysis of the vascular network of bevacizumab treated tumors and of healthy tissues. 6 batches of mice (n = 24 in total) were sacrificed at days 0, 2, 4, 6, 10 and 14 after the beginning of bevacizumab and the tumors were fixed in formalin. The endothelial cells were stained thanks to their expression of CD105 and VEGFR-2, the basal membrane and the pericytes were detected using type IV collagen and desmin, respectively. The pictures on the left represent the tumor vascular network after 10 days of treatment with bevacizumab. The quantification of the blood vessels stained with those four markers was performed on the total tumor tissue surface and is represented as mean +/- SD for each data-point on the graphs. The quantification of the blood vessels on healthy vascular networks is represented in the hatched areas as the mean +/- SD of 4 measures performed on images selected from the Human Protein Atlas of normal human skin biopsies marked with those antibodies (n = 4).

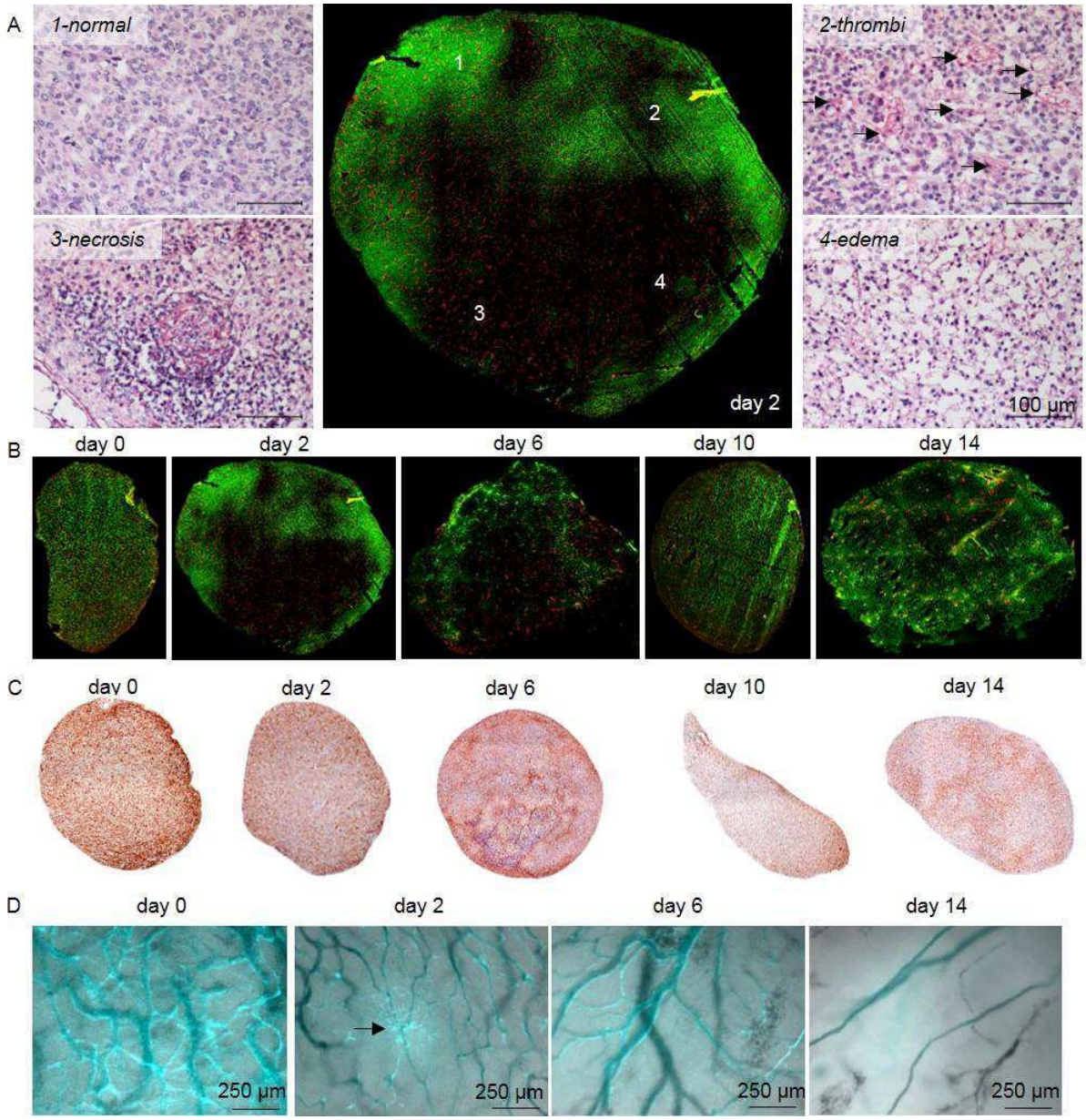

Fig. 6 Vascular and tissue response to bevacizumab treatment. a Evaluation of the perfusion of the tissue of a tumor treated with bevacizumab for 2 days and corresponding HES coloration. The mice received an intravenous injection of Hoechst 33342 (25 mg/kg) 5 minutes before sacrifice and the tumors were salvaged, frozen and immuno-stained for type IV collagen (red). Hoechst 33342 stained cells appear in green and shows the capability of the blood vessels to perfuse the tissue. The HES coloration shows the normal tumor tissue (1), the presence of thrombi in the blood vessels (2, arrows), necrosis (3) and edema (4). b Evolution of the perfusion rate of tumors, untreated (day 0) and treated 2, 6, 10 and 14 days with bevacizumab at 10 mg/kg/day. **c** Evolution of hypoxia in tumors through their expression of the glucose transporter GluT-1. 6 batches of mice (n = 24 in total) were sacrificed at days 0, 2, 4, 6, 10 and 14 after the beginning of bevacizumab and the tumors were fixed in formalin. The expression of GluT-1 in tumors is revealed by the brown coloration of the nuclei in tumors. **d** Evaluation of the vascular permeability *in vivo* without and during bevacizumab therapy. Mice received an intravenous injection of dextran Texas Red R 70 kDa at 10 mg/kg before intravital imaging. The arrow indicates the plasma leakage.